Appendix G

Pillar behaviour

G1 Peak pillar strength evaluation procedures

Stress changes were measured manually on 3D and 2D stress cells, mounted in the hangingwall above six pillars at the three instrumentation sites. Measurements were translated into APS using the Boussinesq equation (Poulos and Davis, 1974) and MinSim 3D numerical models. The form of the equation and an example of the grid configuration used in the Boussinesq analysis is provided as Equation G 1 and Figure G 1 respectively. The stress measurements at the Amandelbult site required a rigorous iterative procedure to untangle the effects of the face and adjacent pillars from the final results. Analyses followed the procedure shown in Figure G 2: Once the APS was established, the Boussinesq solution was again used to determine the influence of possible stress profiles across the pillar on the measurement position. A range of possible stress variation was established for each measurement point.

$$\sigma_{zz} = \sum_{i=1}^{n} \left[\frac{3A_i}{2\pi} \times \frac{z_i^3}{(x_i^2 + y_i^2 + z_i^2)^{5/2}} p_{zi} \right] \qquad \textbf{G 1}$$

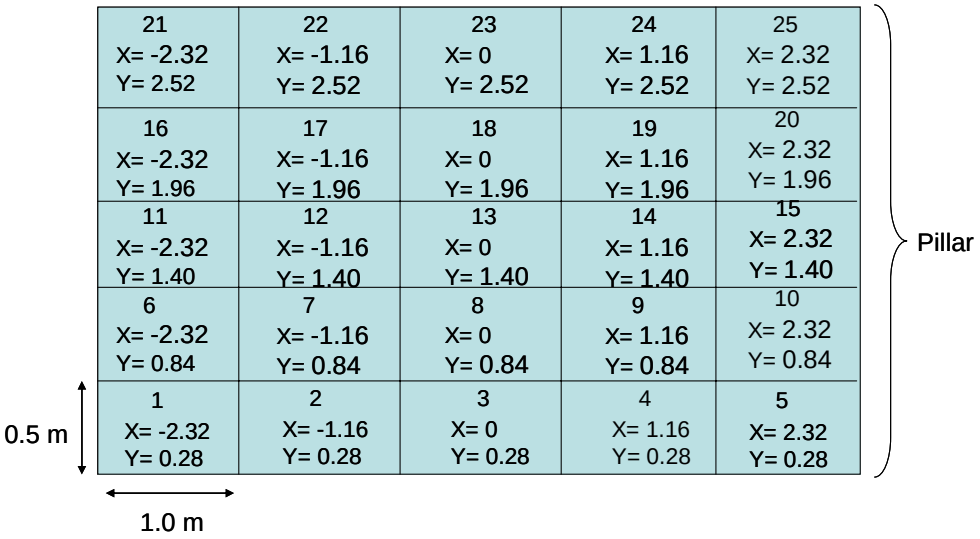

Figure G 1 Typical grid configuration used in the Boussinesq evaluations

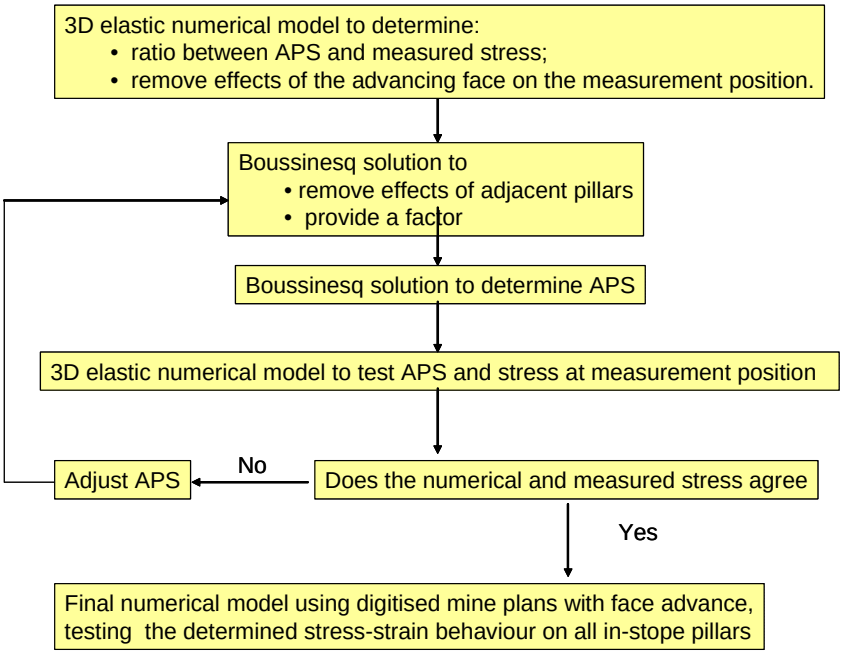

Figure G 2 Flowchart showing the process followed in determining the APS of the instrumented pillars

Separate models were used to analyse each measurement in the stress profiles of Pillars 1 and 2. The models included the face positions of one panel above and

below the pillars of interest. The final configuration used to analyse Pillar 2 is shown as an example in Figure G 3. Stress conditions were artificially assigned to account for the workings around these panels. For completeness the final results were checked against a model using digitised plans of the area. The stress evaluations at the Impala and Union sites were less complicated and reasonable evaluations were possible with only the MinSim 3D numerical models and digitised plans.

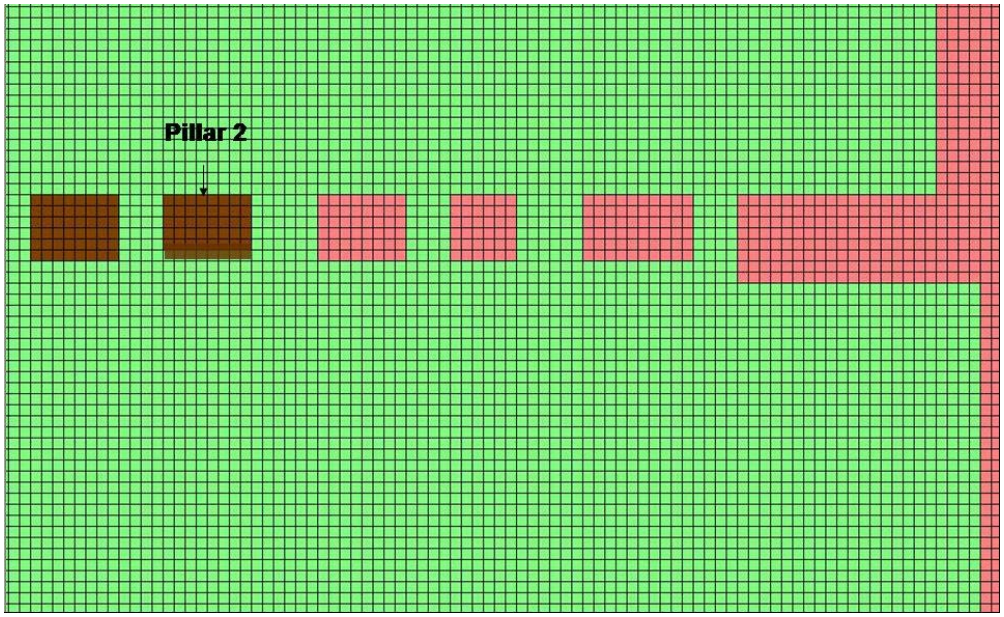

Figure G 3 Numerical model layout used to determine the Pillar 2 APS

All the analyses were performed assuming that the behaviour of adjacent pillars were the same as the measured pillar. The likely variation in stress profiles of adjacent pillars will introduce small errors if the stress change measurements were conducted relatively close to the pillar such as Amandelbult P1. However, at greater height such as Amandelbult P2 the measurements were significantly affected by the surrounding pillars, particularly before the adjacent pillar failed. The evaluations of these effects are described below:

The analysis conducted on Amandelbult P1 suggest that the stope face had advanced sufficiently far from the 3.5 m high measurement position over the pillar at the time of installation so that the stress influence of the stope face could be ignored. The stress contribution from adjacent pillars to the analysis was low as

shown in Figure G 4. The likely error if the adjacent pillar has not failed is about 15% and this would only affect post-peak results, i.e. the slope of the stress-strain curve. The influences of these pillars were subtracted from the results using the procedure described in Figure G 2. The relative closeness of the measurement point above Amandelbul P1 (3.5 m above the pillar) introduces other errors though, associated with potential stress profiles across the pillar. A range of between an overestimate of 25 per cent before failure to an underestimation of 49 per cent in the post failure region is shown in Table G 1 and Figure G 5. Some of the investigated scenarios are extreme and unlikely and a more probable range is between 12 per cent and 24 per cent for the pre and post failure scenarios respectively. The likely errors in the post failure measurements are shown between the dashed lines in Figure G 5. Note that the pre-failure measurement is likely to be overestimated while the post-failure results could be underestimated.

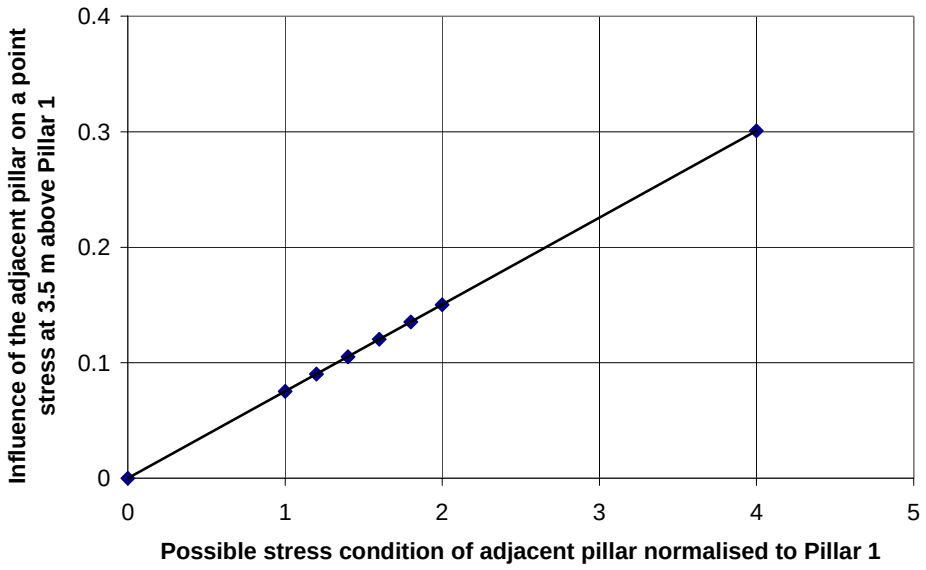

Figure G 4 Effect of adjacent pillars on P1 measurements

Table G 1 Errors associated with possible stress profiles across P1

Stress condition	**Profile number (used in** Error! Reference source not found.**)**	**Stress profile across Pillar 1 normalised to APS (wide to narrow end)**	**Percentage error**
Pre-fail worst	0	1.5:1.5:0	-25%
Pre-fail likely	1	1.25:1.25:0.5	-12%
Pre-fail normal	2	2:0:2	-2%
Post-peak normal	3	0:3:0	4%
Post-peak measured	4	2.07:0.34:0.59	24%
Post-peak worst	5	0:0:3	49%

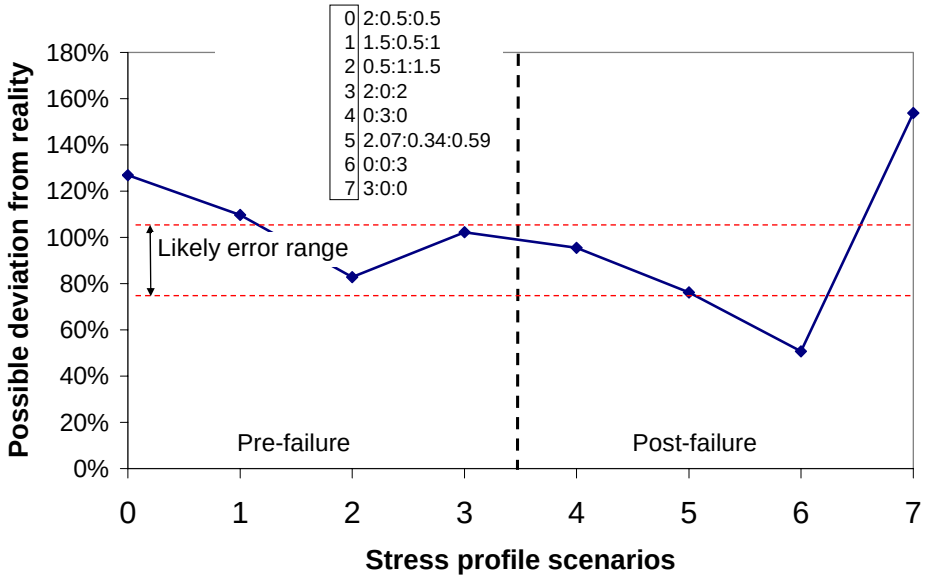

Figure G 5 Synopsis of potential errors associated with stress profiles across P1

The evaluations conducted on Amandelbult P2 at a height of 6.5 m showed that the effects of adjacent pillars on the measurements were significant as illustrated in Figure G 6. A sensitivity analysis indicated errors of up to 43 per cent if it is assumed that an adjacent pillar was carrying double the stress of the monitored pillar. The procedure described in Figure G 2 allowed the identification and removal of the face effects and therefore the analysis of the peak strength. However, the post failure stress drop results are uncertain and the analyses of the data assume equal residual strength on the adjacent pillars. This assumption appears reasonable as visually the pillars were similar and about the same size and shape. The errors associated with the possible stress profiles across the pillar (Table G 2) were much less than for Pillar 1, and the likely range shown in Figure G 7 indicates a possible overestimate of about 6 per cent.

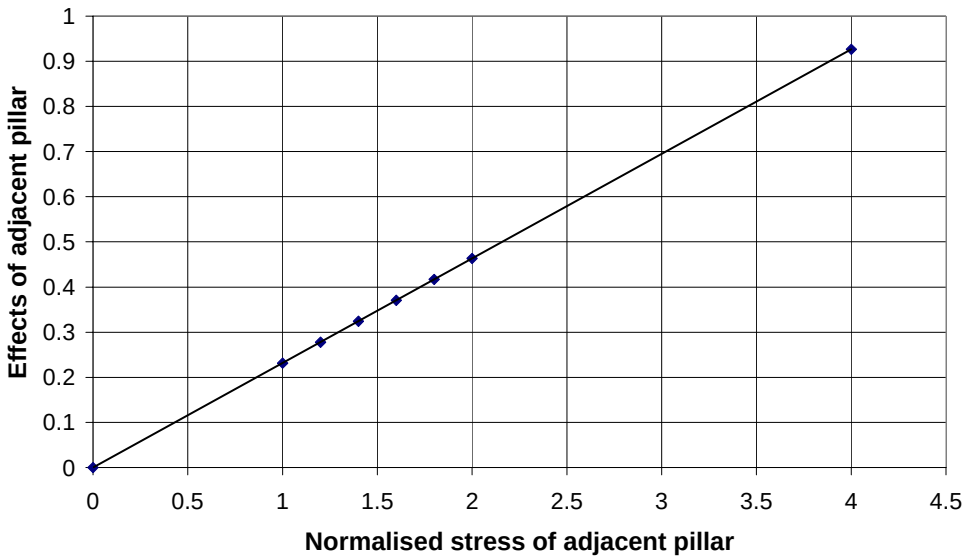

Figure G 6 Effect of adjacent pillars on P2 measurements

Table G 2 Errors associated with possible stress profiles across P2

Stress condition	Profile number (used in Error! Reference source not found.)	Stress profile across Pillar 2 normalised to APS (wide to narrow end)	Percentage error
Pre-fail worst	0	1.5:1.5:0	106
Likely	1	1.25:1.25:0.5	106
Pre-failure	2	1.5:0:1.5	99
Peak middle	3	0:3:0	101
Measured	4	0:1.9:1.1	109
Peak wide end	5	0:0:3	77
Peak narrow end	6	3:0:0	121

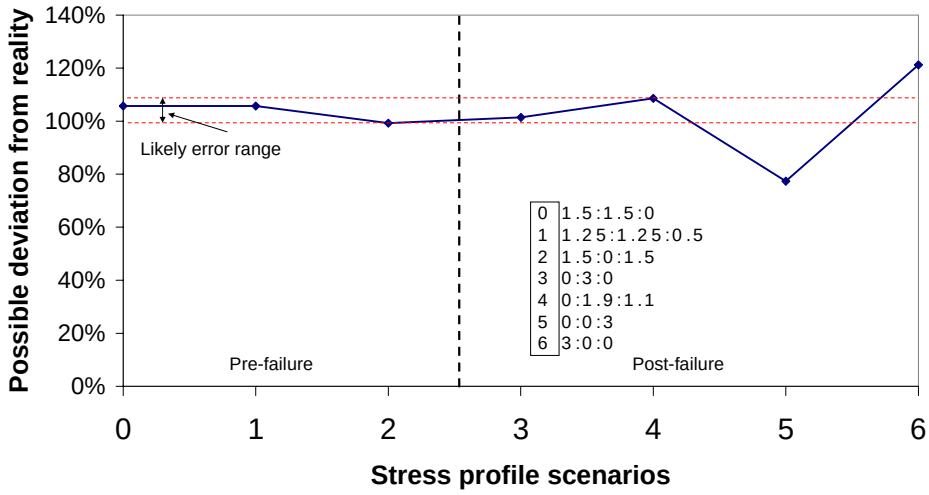

Figure G 7 Synopsis of potential errors associated with stress profiles across P2

Finally, the peak strengths of the pillars were compared to a linear pillar strength formula derived using Maximum Likelihood back analysis on pillars from Impala Platinum (Chapter 5.3). The effective width-to-height ratios of pillars without sidings were evaluated using Equation G2 (Roberts et al, 2002).

$$h_e \approx \left[1 + 0.2692(w/h)^{0.08}\right]h \qquad \textbf{G2}$$

G2 Residual strength analysis

Residual stress measurements were made at regular intervals from shallow-dipping boreholes drilled across the top of the instrumented pillars. The evaluations were done after the pillars had reached their residual state, as indicated by the stress change measurements.

Most of the residual stress measurements were made using 2D doorstopper instruments. The results reflect stresses in the plane of the pillar long-axis in the sub-vertical and horizontal directions (Figure G 8). Only the sub-vertical stresses were used in the average pillar strength (APS) evaluations. The extrapolated stress distributions across the pillars were calculated using a 'best fit', inverse matrix of Boussinesq equations (Equation G 1). An example of a typical matrix grid that was employed in the evaluations is shown in Figure G 1. The equation assumes that the host rock is linear elastic.

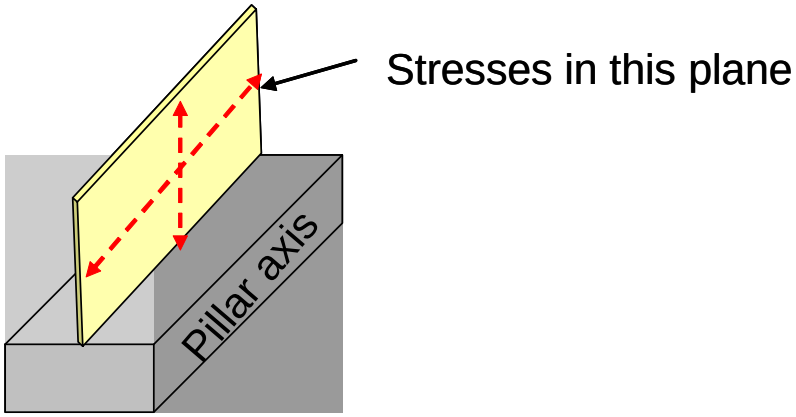

Figure G 8 Sketch of a pillar showing the plane in which the 2D residual stress measurements were made

G3 Amandelbult 1-Shaft

G3.1 Stress change measurements

G3.1.1 Stope sheet

The stope sheet in Figure G 9 shows the approximate locations of the stress cells and closure meters used to measure the behaviour of Pillars P1 and P2 at Amandelbult. The stress change cell above P1 was installed about 2.2 m behind the down-dip face (Panel 13-16-2E) while the cells above P2 were installed 1.3 m ahead and 0.82 m behind the face respectively. All the closure stations were installed ahead of the face.

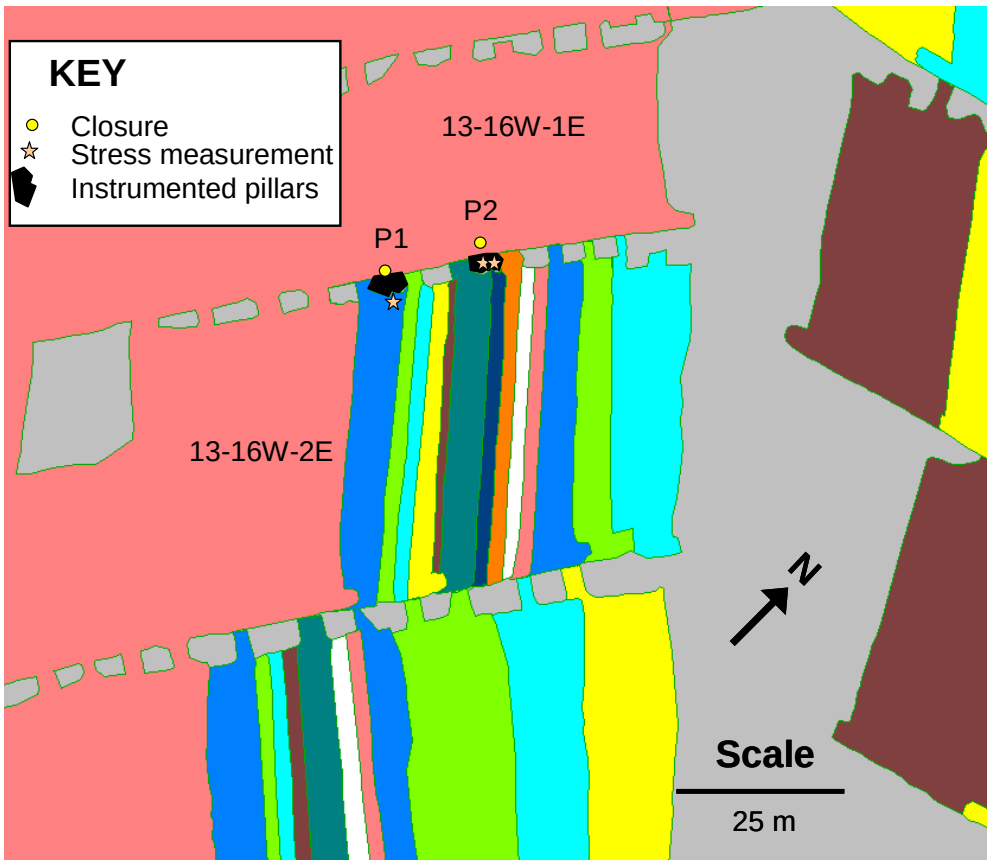

Figure G 9 Stope sheet showing the positions of the stress-change cells and closure meters at the Amandelbult site

G3.1.2 Pillar P1 - section and plan view

A section and plan view showing the orientation of the instrument installed over P1 is shown in Figure G 10 and Figure G 11, respectively.

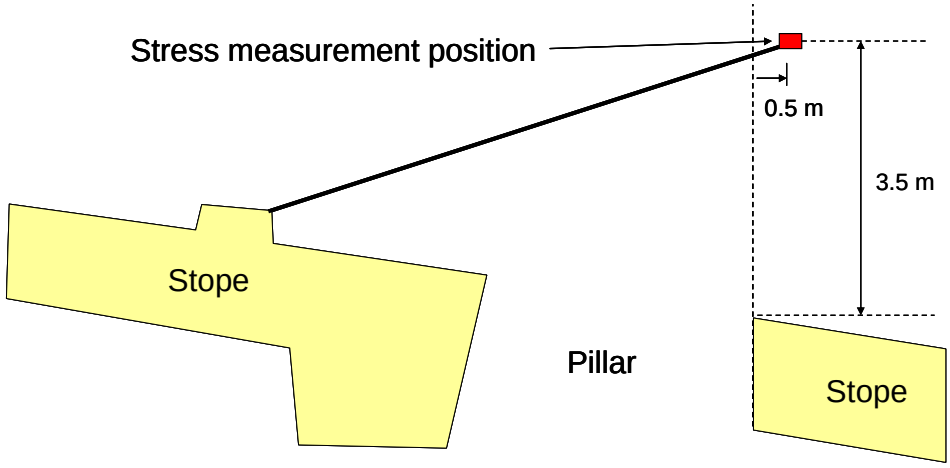

Figure G 10 Section showing the instrumentation position above Amandelbult P1

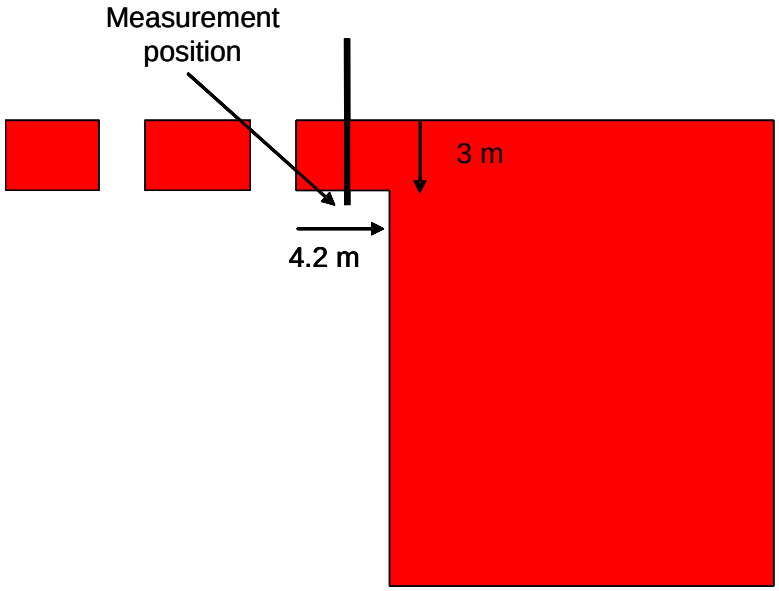

Figure G 11 Plan view of Amandelbult P1 at cell installation

The final shape and size of Pillar 1 was determined by off-set measurements made underground after the panel had reached its limit and is shown in Figure G 12. On average the pillar is 2.5 m wide and 5.5 m long with an average stoping width of 1.1 m.

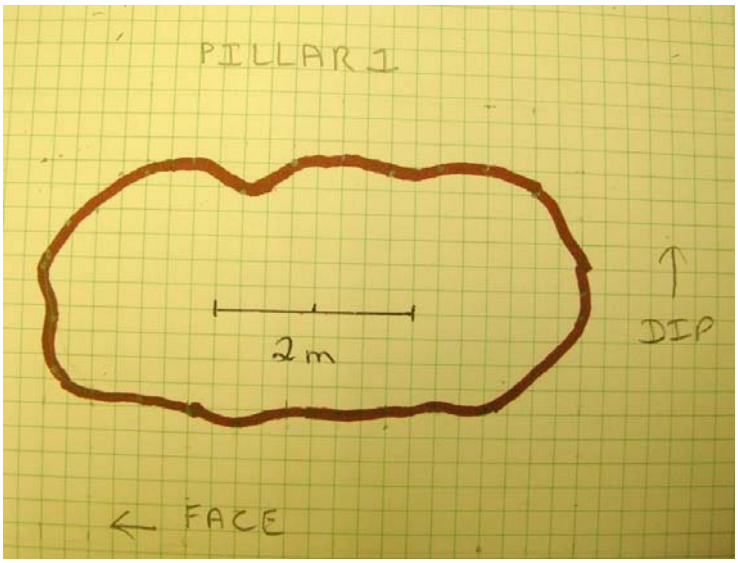

Figure G 12 Plan view showing the size and shape of Amandelbult P1

G3.1.3 Pillar P2 – section and plan view

P2 (Figure G 9) is slightly wider and shorter than the final dimensions of P1. The plan view shown in Figure G 13 was also drawn using off-set measurements made underground and shows the average width and length as 3 m and 4.3 m respectively. The average stoping width is 1.1 m, providing an effective width to height ratio of 2.2 if Equation G2 is applied.

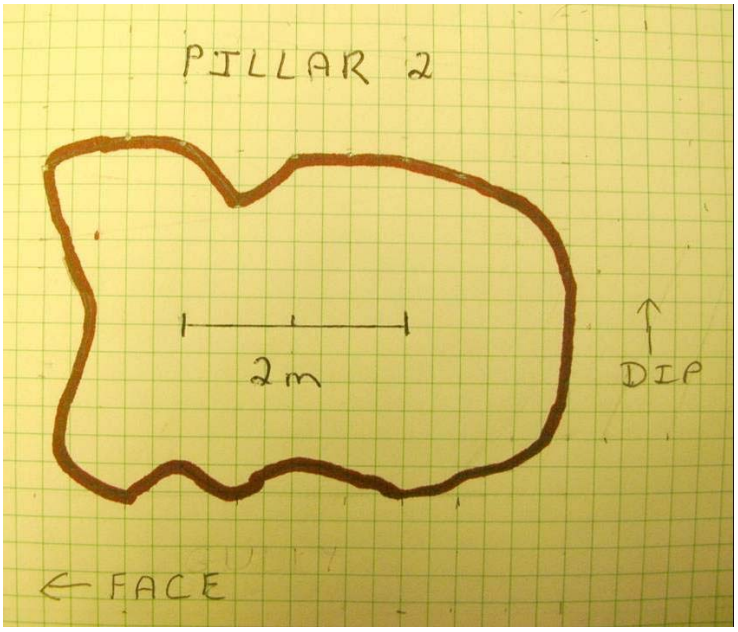

Figure G 13 Plan view showing the size and shape of Amandelbult P2

Two stress change cells were installed above P2. A 3D CSIRO cell was mounted at a height of 6.5 m (1 in Figure G 14 and Figure G 15) and 1.3 m ahead of the down-dip face, i.e. prior to pillar formation (Figure G 15). The other instrument was a 2D doorstopper, mounted at a height of 6.3 m above the pillar, and 0.82 m behind the down-dip face (2 in Figure G 14 and Figure G 15). The face position at the installation of this cell is shown by the dotted line in Figure G 15. A 2D field stress measurement was performed just behind the final cell position and this result was used in the back analysis of the P2 average pillar stress (APS).

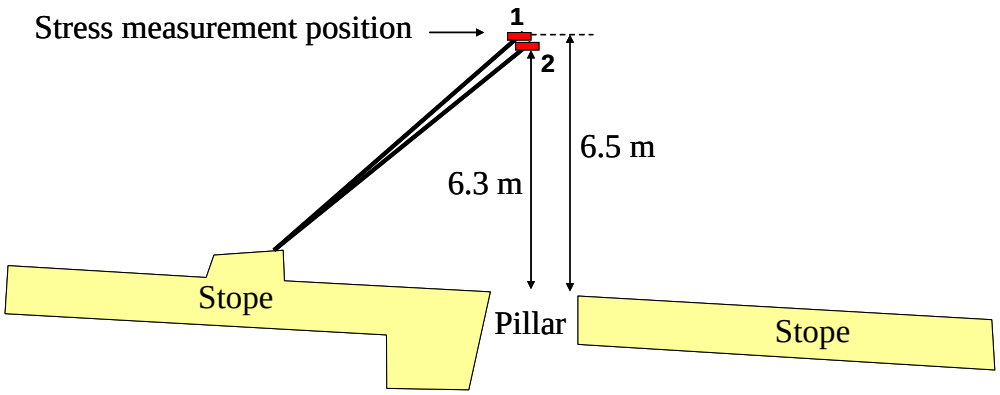

Figure G 14 Section showing the instrumentation position above P2

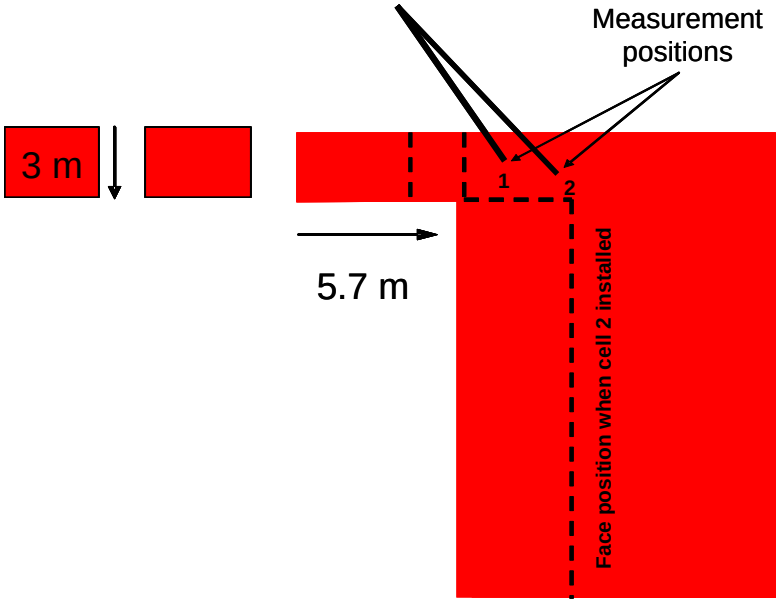

Figure G 15 Plan view of the cell installations over P2

G3.2 Residual strength measurements

Residual stress measurements were conducted at regular intervals across the top of the two instrumented pillars after the faces of the panels above and below these pillars had reached their limit and had stopped mining. This investigation included P1 and P2 (Figure G 16). The measurements were conducted from boreholes drilled up at 23° to the strata (5° above horizontal) as shown in Figure G 17.

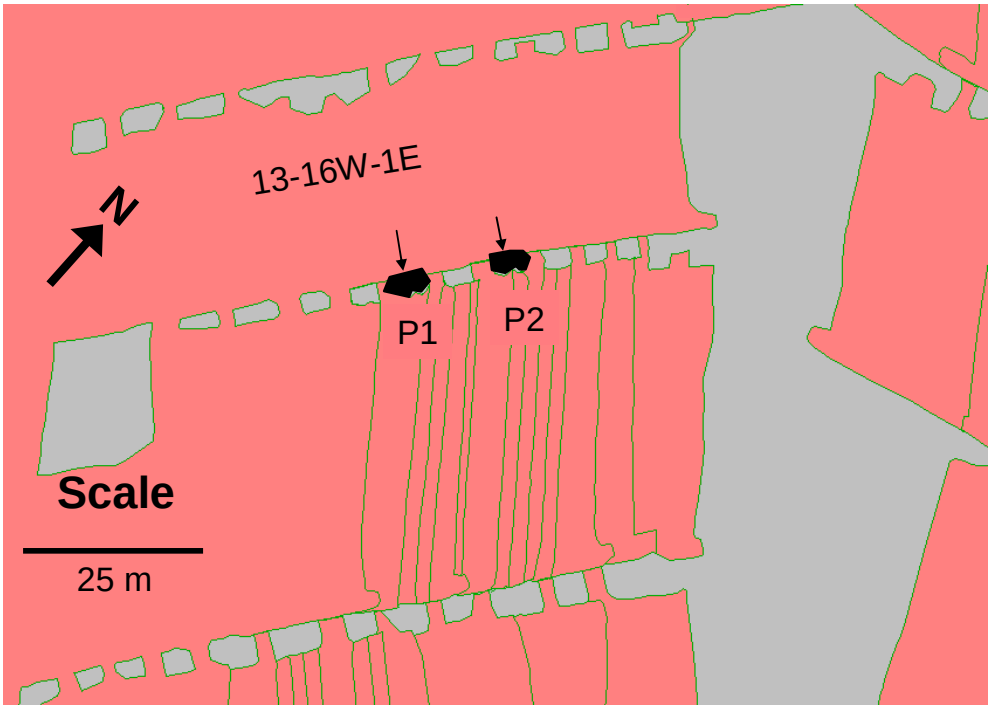

Figure G 16 Stope sheet showing the crush pillars over which stress profile measurements were made at Amandelbult

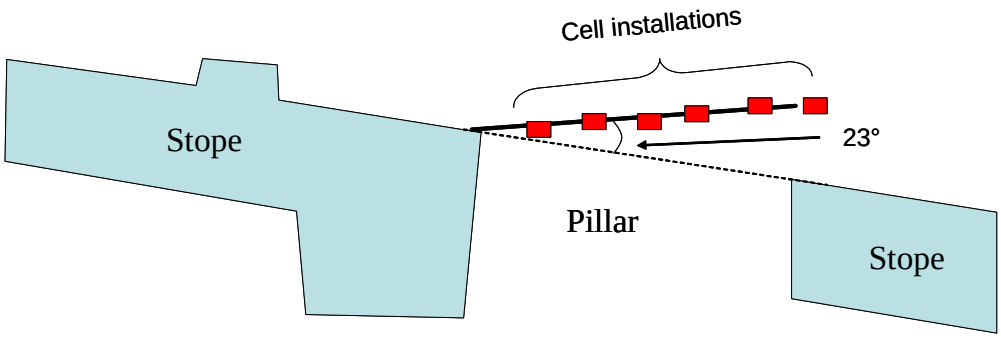

Figure G 17 Section showing the measurement positions over Amandelbult P1 and P2 after pillar failure (not drawn to scale)

Most of the residual stress measurements were made using 2D doorstopper instruments. The results reflect stresses in the plane of the pillar long-axis in the sub-vertical and horizontal directions (Figure G 18). Only the sub-vertical stresses are shown in Figure G 19.

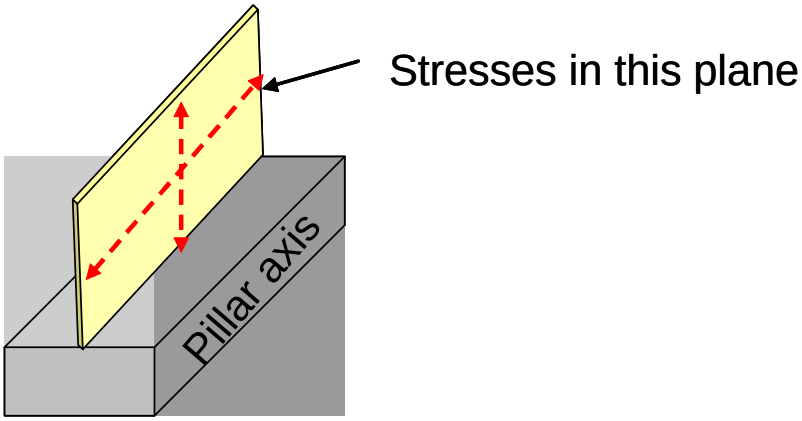

Figure G 18 Sketch of a pillar showing the plane in which the 2D residual stress measurements were made

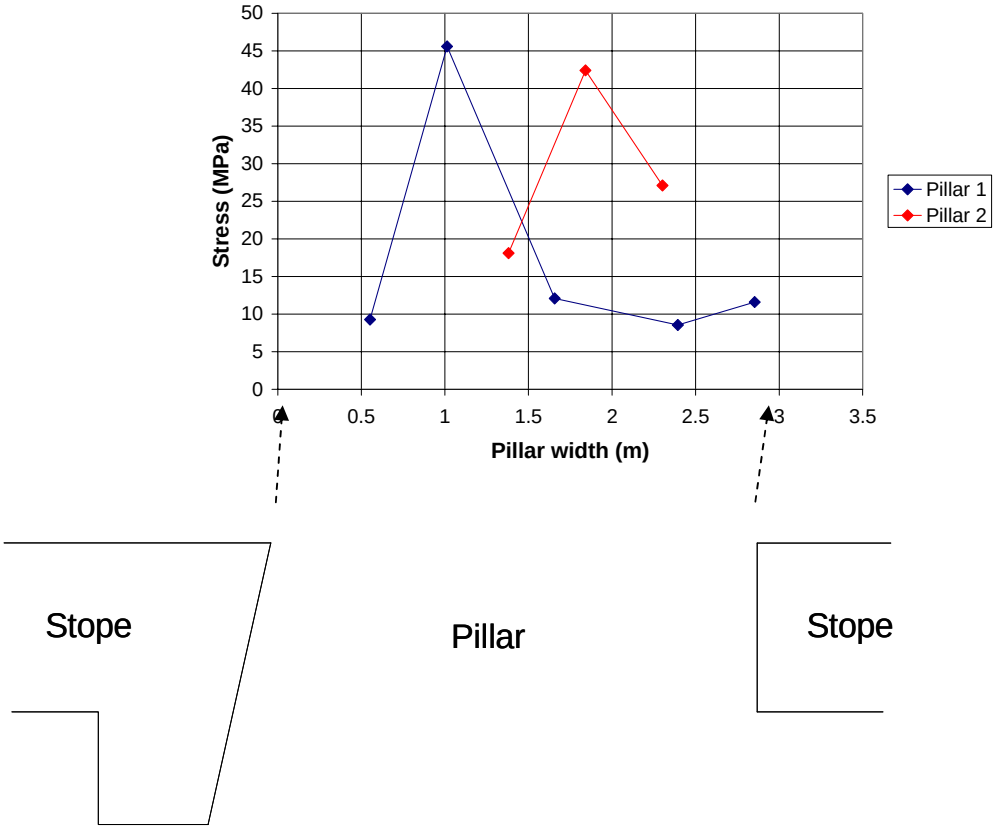

Figure G 19 Stress profile across two failed pillars (not corrected for measurement height) and a sketch of a 3 m wide pillar

For the purposes of the calculations, the reef and measurements were rotated by 18° so that the top surface of the pillars could be considered horizontal. Plan views of the Boussinesq co-ordinate system used across the top boundaries of the pillars are shown in Figure G 20 and Figure G 21 for P1 and P2 respectively. The grid enabled multiple stresses to be considered across the pillar. The reference point used for the evaluation of the stress measurements was the centre of the up-dip edge of the pillar (the bottom edge of the grid layouts). In both instances the matrix inversion of the measured stresses provided an unrealistic profile of pillar stresses. It was therefore necessary to a 'best fit' profile and the estimated stress distribution across the pillar was estimated from this profile.

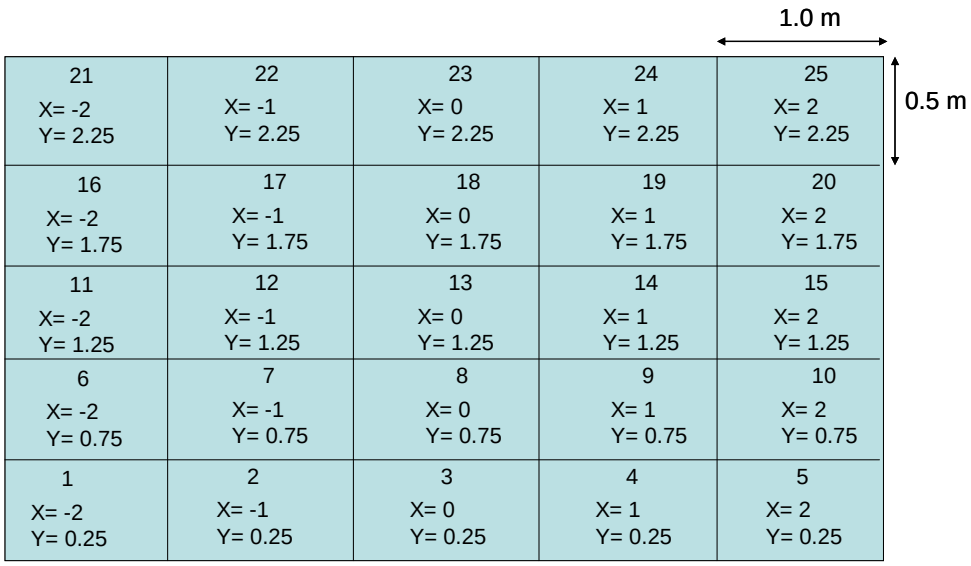

Figure G 20 Plan view of the grid layout across P1 for the Boussinesq evaluation. The origin is the centre of the bottom (down-dip edge)

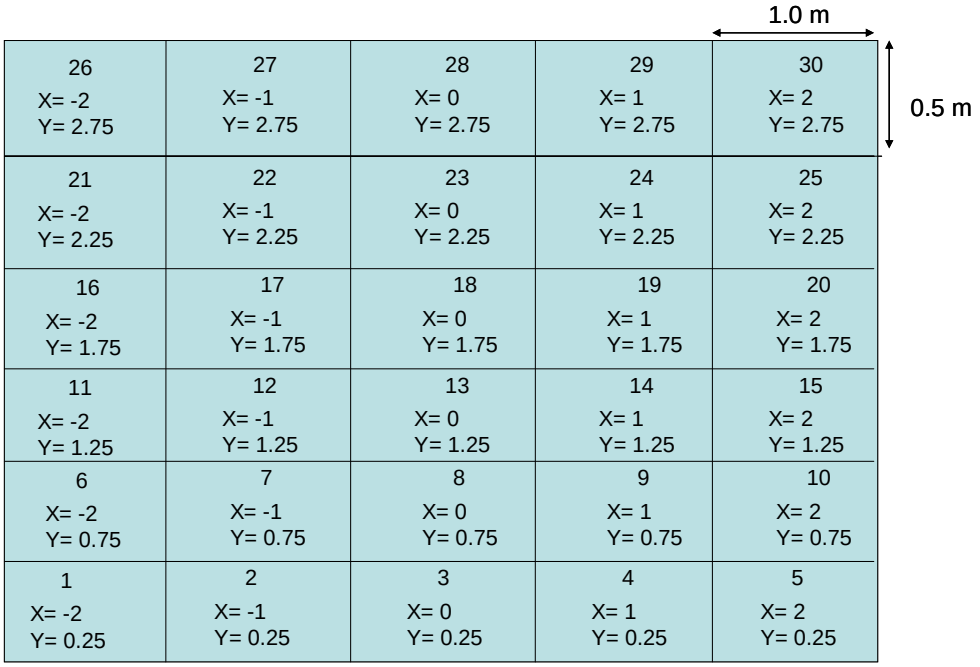

Figure G 21 Plan view of the grid layout across P2 for the Boussinesq evaluation. The origin is the centre of the bottom (down-dip edge)

G4 Impala 10-shaft

G4.1 Stress change measurements

G4.1.1 Stope sheet

Measurements were conducted on three different size pillars, marked P1 to P3 in Figure G 22. Mining operations were temporarily stopped in Panel 8s when the face was in line with the centre of P2. During this time the ASG was extended beyond P3, holings were cut to the north of P1 and between P1 and P2 and a siding was cut on the up-dip sides of P2 and P3. At the time when the 8s face was stopped, the siding was about 9 m behind the face and a piece was cut from the north side of P1. P1 failed just before the 8s face stopped at dimensions of 5.6 m x 6.8 m (dip x strike). P2 appears to have failed when the holing between

P1 and P2 was completed. The pillar was about 6.0 m x 5.5 m (dip x strike) at this stage. P3 failed during the cutting of the siding at dimensions of 4 m x 3.6 m (dip x strike).

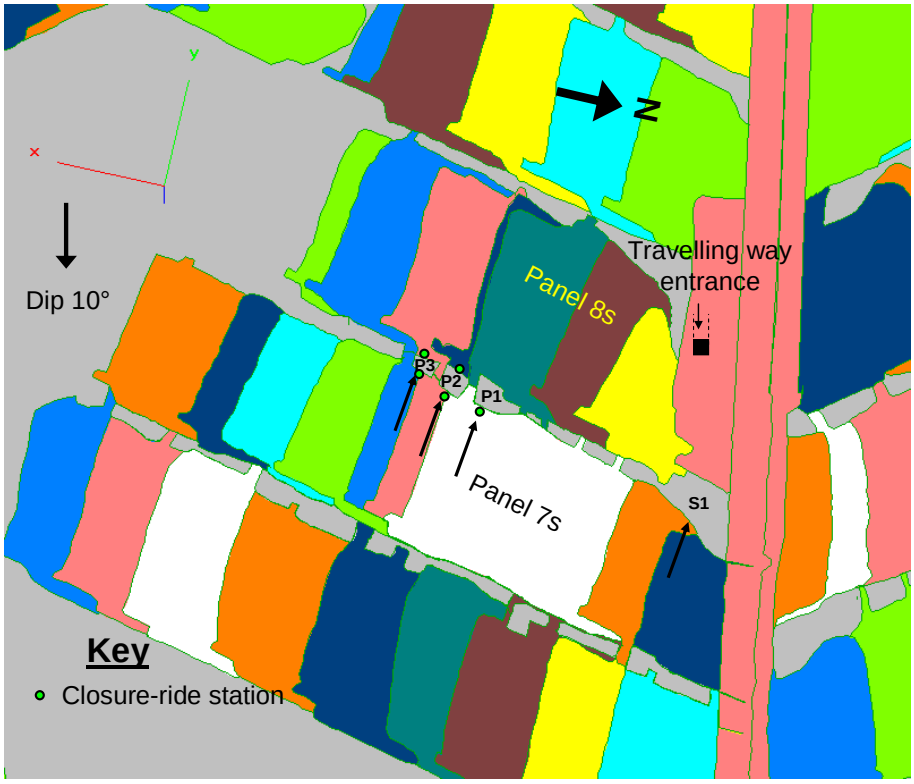

Figure G 22 Stope sheet showing the monitored pillars

Closure-ride stations were installed on the down-dip side of all three pillars and on the up-dip sides of P2 and P3. The fractured rock fragments fallen from the pillar edge and the unstable hangingwall conditions adjacent to P1 prevented the stations from being installed at the pillar edge on the down-dip sides of P1 and P2. Measurements were thus made at about 1 m and 2 m from P1 and P2 respectively.

G4.1.2 Pillar P1 - section

Stress change measurements were conducted at 5.28 m above and 0.74 m from P1 as shown in Figure G 23. A field measurement was conducted in a separate borehole and the stress adjusted to provide a starting stress. The estimated peak

stress was compared to an elastic, MinSim model assuming the face positions at the time of pillar failure. A good comparison was achieved when the small pillars were given a residual of 20 MPa. A set of conversion factors were determined to subtract out the effects of the face by comparing the modelled pillar stress to a benchmark at the position of the measurements and advancing the 8s panel until the effects of the face could no longer be measured. After the stress on the pillar dropped to residual levels a second field measurement was conducted and the stresses adjusted for the now non-linear rock behaviour. The residual stress was adjusted according to this measurement. Note that the rock in which the measurements were made became non-linear when the pillar dropped suddenly to the residual state (Chapter 3) and additional strain was measured. If this strain was included in the calculations, the predicted final pillar stress would have been tensile.

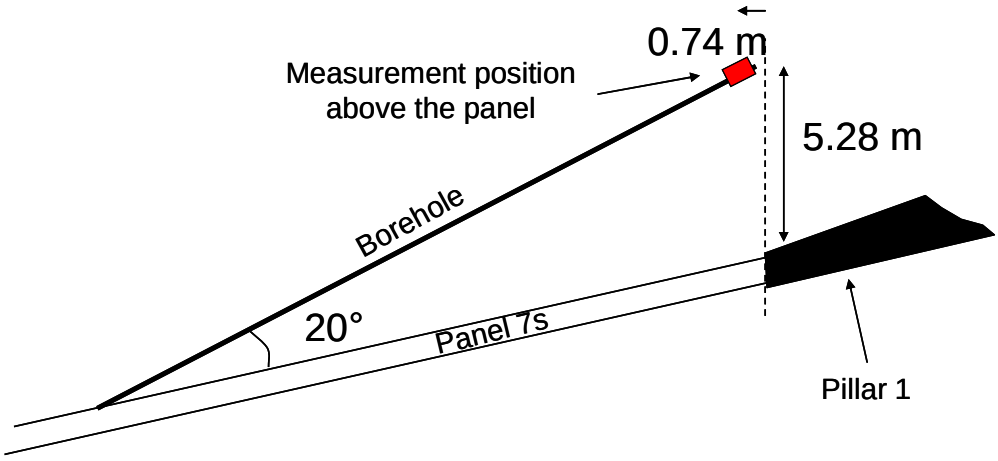

Figure G 23 Section showing the stress cell position above P1 (not drawn to scale)

G4.1.3 Pillar P2 - section

Measurements were conducted from a hole drilled through the centre of the pillar from the haulage below (Figure G 24) and from a shallow dipping borehole drilled from the stope (Figure G 25).

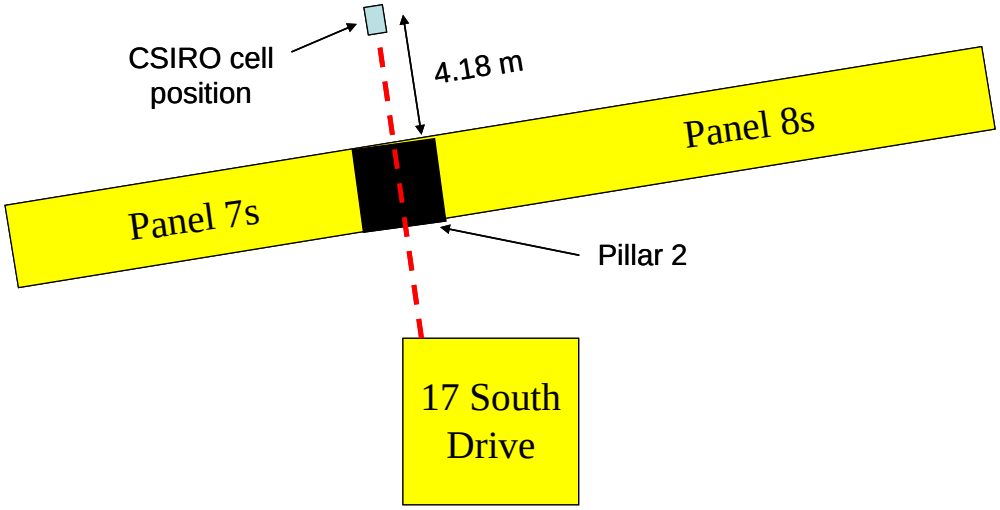

Figure G 24 Diagram showing the position of the CSIRO cell above P2 (not drawn to scale)

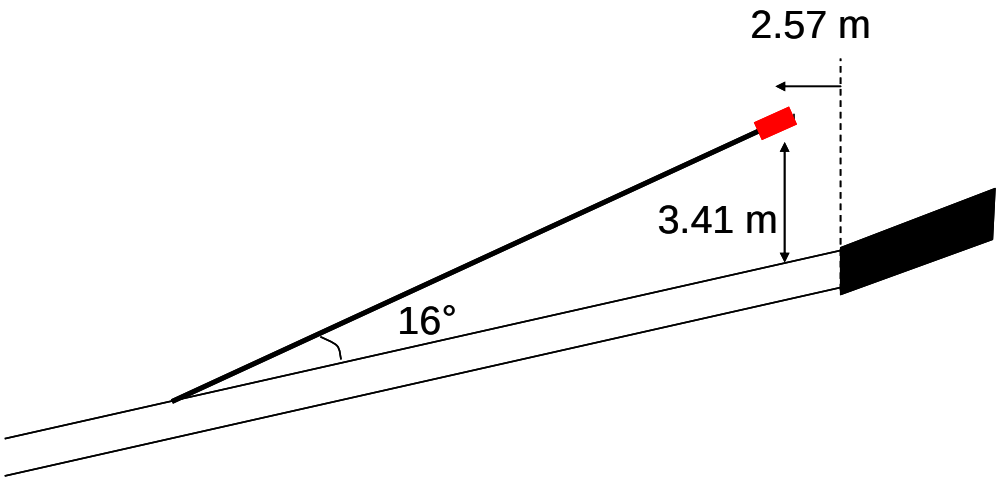

Figure G 25 Diagram showing the position of the doorstopper cell above Impala P2 (not drawn to scale)

The methodology applied to convert the measured stress to APS in the Impala P1 study was also used in the Impala P2 evaluation. Unfortunately the cable extending from the CSIRO cell was damaged when the pillar failed and no further readings were possible. However, the doorstopper was installed before pillar failure and there was an overlap. Different factors were required to evaluate the

two sets of data, but both appear to predict about the same peak strength, which was also similar to the MinSim model.

The errors due to the most likely stress profiles across the pillar on the measurement point are shown in Figure G 26. A maximum error of 9% is indicated.

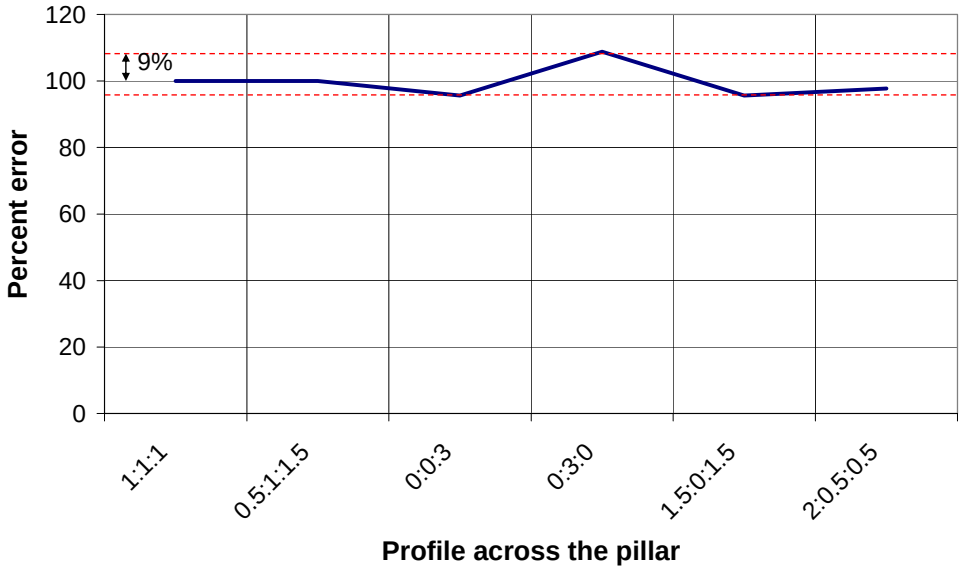

Figure G 26 Synopsis of potential errors associated with stress profiles across Impala P2

G4.1.4 Pillar P3 - section

The measurements were made 3.23 m above the stope and over the down-dip edge of Pillar 3 as shown in Figure G 27. The field stress was measured just behind the stress change cell in the same borehole.

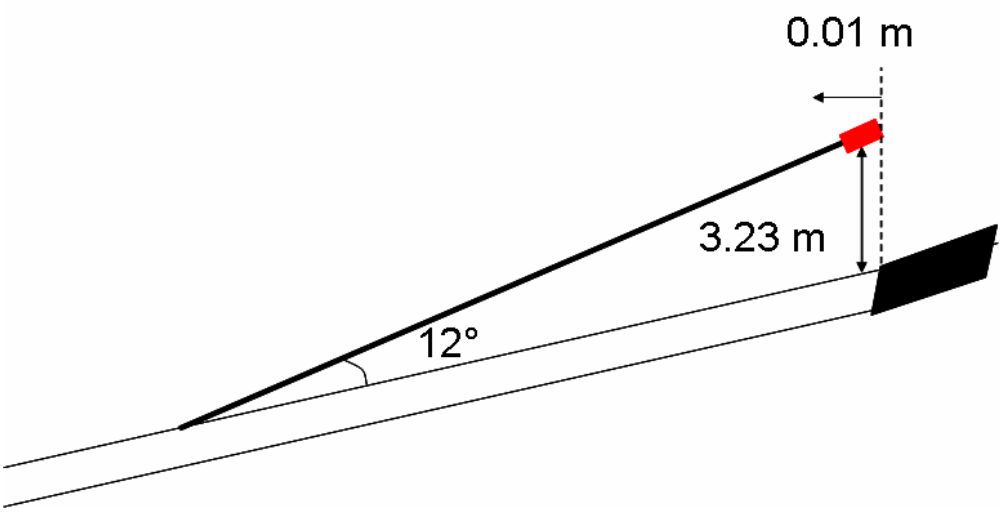

Figure G 27 Section showing the position of the doorstopper cell above Impala P3 (not drawn to scale)

G4.2 Residual strength measurements

G4.2.1 Pillar P1 – section and plan view

The final pillar size was approximately 4.8 m long and 5.2 m wide with a narrow, highly fractured strip on one side. A series of field stress measurements were conducted in two shallow dipping boreholes (~15° steeper than the reef) drilled about 1.9 m and 3.6 m above the centre of the pillar. A section through the pillar is provided in Figure G 28 to show the approximate measurement positions of the lower borehole. The upper borehole had a similar dip but was collared further back from the pillar.

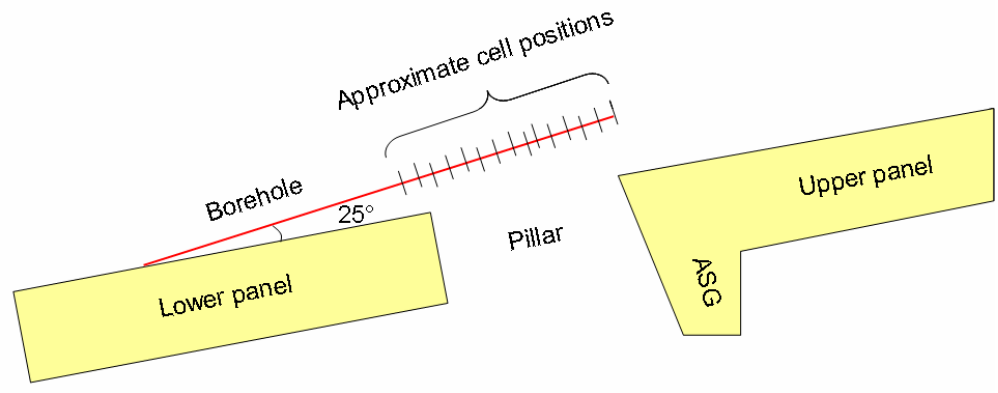

Figure G 28 Section showing the asymmetric shape of Impala P1 and the approximate stress cell positions in Borehole P1a (not to scale)

For the purposes of the calculations, the reef and measurements were rotated by 10° so that the top surface of the pillar could be considered horizontal. A plan view of the Boussinesq co-ordinate system used across the top boundary of the pillar is shown in Figure G 29. The grid enabled multiple stresses to be considered across the pillar. The matrix inversion of the measured stresses provided an unrealistic profile of pillar stresses at this site. It was therefore necessary to invert a 'best fit' to the anticipated stress distribution across the pillar, guided by the measured profile and the APS measured by the stress-change instrument.

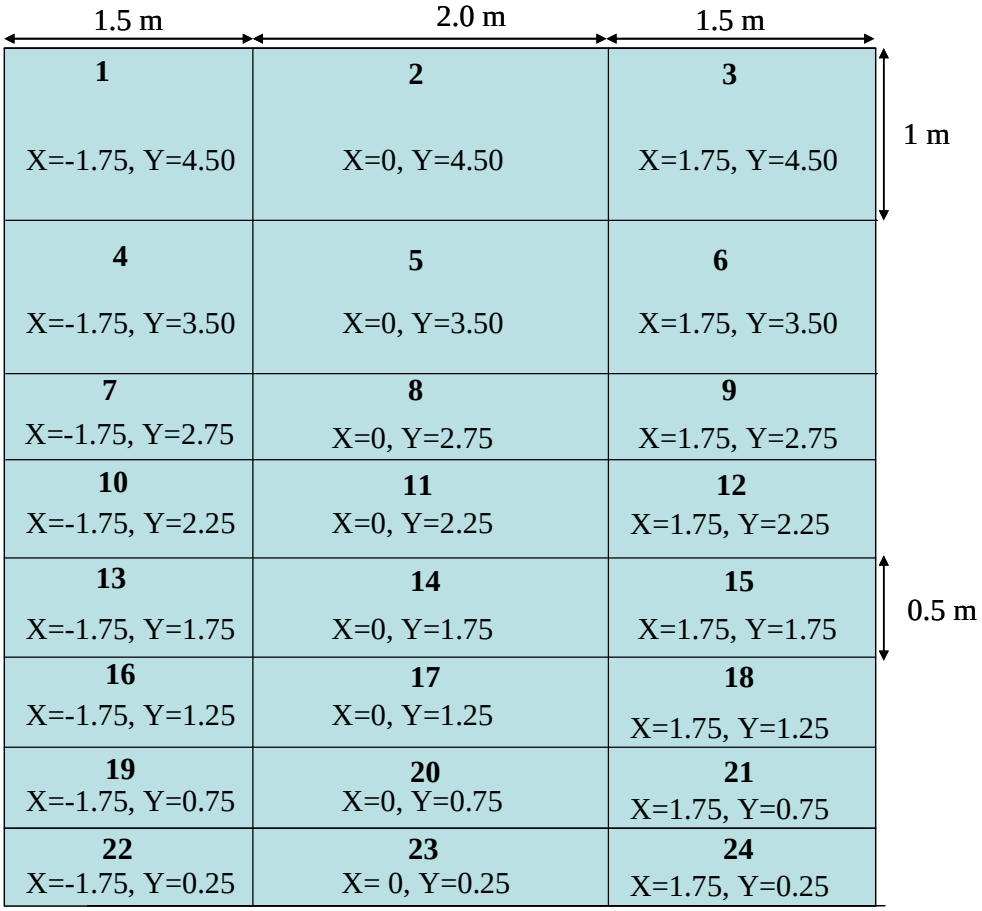

Figure G 29 Plan view of the grid layout across Impala P1 for the Boussinesq evaluations. The origin is the centre of the bottom (down-dip edge)

G4.2.2 Pillar P2 – section and plan view

Two parallel boreholes were drilled at 10° to the strata to measure the field stress conditions at close intervals (Figure G 30). The boreholes collared at the same distance from the pillar, spaced approximately 0.5 m apart. Most of the instruments measured 2D stress but a triaxial cell was installed in P2b to determine the axial stress. A third borehole was drilled at 15° to the strata and a series of eight triaxial cells were installed.

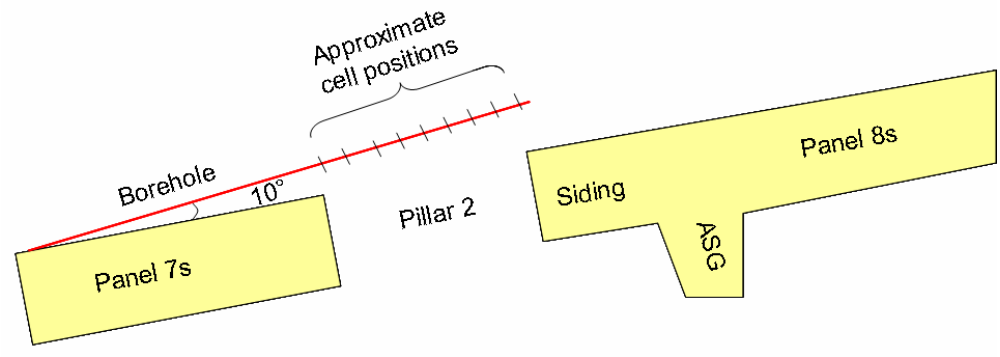

Figure G 30 Section showing Impala P2 with the approximate stress cell positions in Borehole P1a (not to scale). P2b was parallel to P2A

The reef and measurements were rotated by 10° so that the top surface of the pillar could be considered horizontal for the purposes of the Boussinesq evaluation. A plan view of the Boussinesq co-ordinate system used across the top boundary of the pillar is shown in Figure G 31. A 'best fit' average of the measured stress from the two parallel boreholes (P2a and P2b) was used in the matrix inversion. The estimated stress distribution across the pillar was estimated from this 'best fit' profile.

21 X= -2 Y= 3.15	22 X= -1 Y= 3.15	23 X= 0 Y= 3.15	24 X= 1 Y= 3.15	25 X= 2 Y= 3.15
16 X= -2 Y= 2.45	17 X= -1 Y= 2.45	18 X= 0 Y= 2.45	19 X= 1 Y= 2.45	20 X= 2 Y= 2.45
11 X= -2 Y= 1.75	12 X= -1 Y= 1.75	13 X= 0 Y= 1.75	14 X= 1 Y= 1.75	15 X= 2 Y= 1.75
6 X= -2 Y= 1.05	7 X= -1 Y= 1.05	8 X= 0 Y= 1.05	9 X= 1 Y= 1.05	10 X= 2 Y= 1.05
1 X= -2 Y= 0.35	2 X= -1 Y= 0.35	3 X= 0 Y= 0.35	4 X= 1 Y= 0.35	5 X= 2 Y= 0.35

Figure G 31 Plan view of the grid layout across Impala P2 for the Boussinesq evaluations. The origin is the centre of the bottom (down-dip edge)

G4.2.3 Pillar P3 – section and plan view

A total of 11 stress measuring instruments were installed in two boreholes drilled above P3 (Figure G 32). In plan the boreholes were drilled across the narrow section of the pillar from the centre of the long axis (Figure G 33). Nine biaxial cells (Doorstoppers) and one CSIR triaxial cell were installed in a shallow-dipping borehole (15° steeper than the reef), drilled from the down-dip panel. Two CSIR triaxial cells measured the 3D stress conditions from a steeply dipping borehole drilled from the up-dip panel.

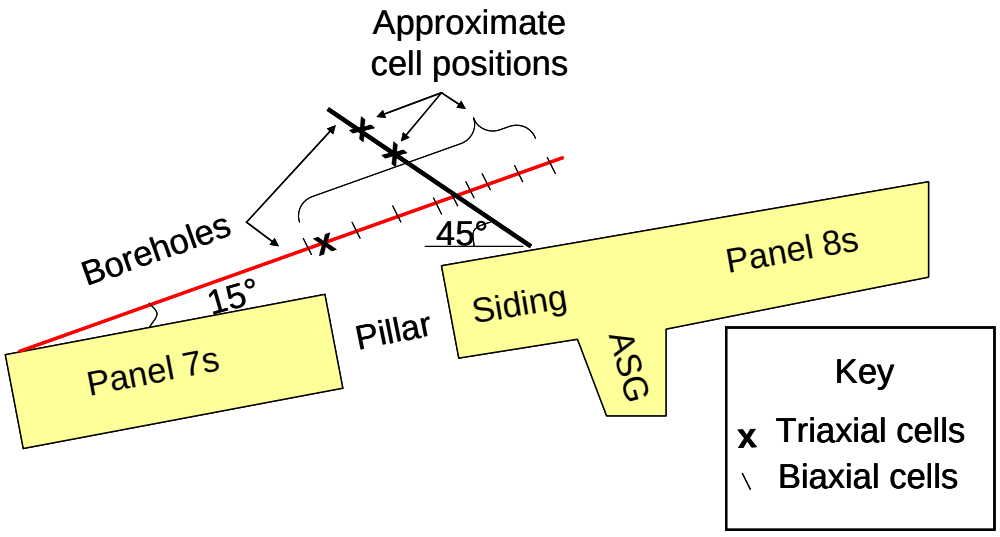

Figure G 32 Section showing the instrumentation positions above Impala P3 (not drawn to scale)

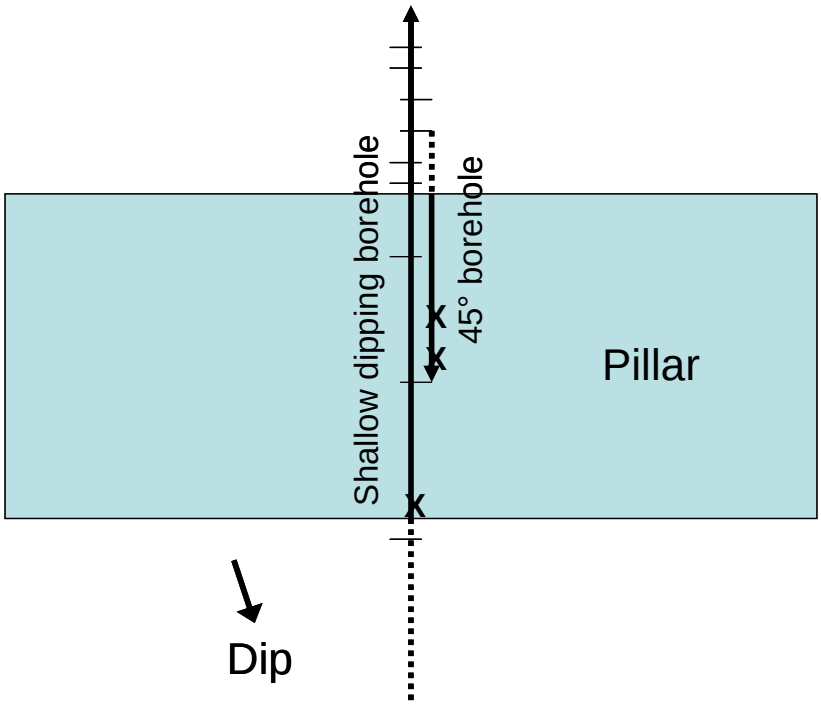

Figure G 33 Plan view showing the instrumentation positions above Impala P3 (not drawn to scale). X=triaxial cells, - =biaxial cells

The measurements in the shallow-dipping hole ranged in height from 1.9 m to 3.7 m above the pillar. The intention was to measure vertical stress with a set of closely spaced cells. However, two obliquely oriented, vertical discontinuities prevented some measurements. The two triaxial cells in the 45° borehole were installed at heights of 3.7 m and 4.2 m above the pillar. These measurements allowed a much broader overview of the stress condition of the whole pillar, by virtue of their height above the pillar. The stress distribution across the pillar itself was calculated using an inverse matrix of Boussinesq equations (Poulos and Davis, 1974), based on the measurements in the shallow-dipping borehole. The measurements conducted in the 45° borehole were subsequently used to check the evaluated pillar stress profile. For the purposes of the calculations, the reef and measurements were rotated by 10° so that the top surface of the pillar could be considered horizontal. A plan view of the Boussinesq co-ordinate system used across the top boundary of the pillar is shown in Figure G 34. The pillar was divided into 0.5 m x 0.5 m blocks as shown in the figure.

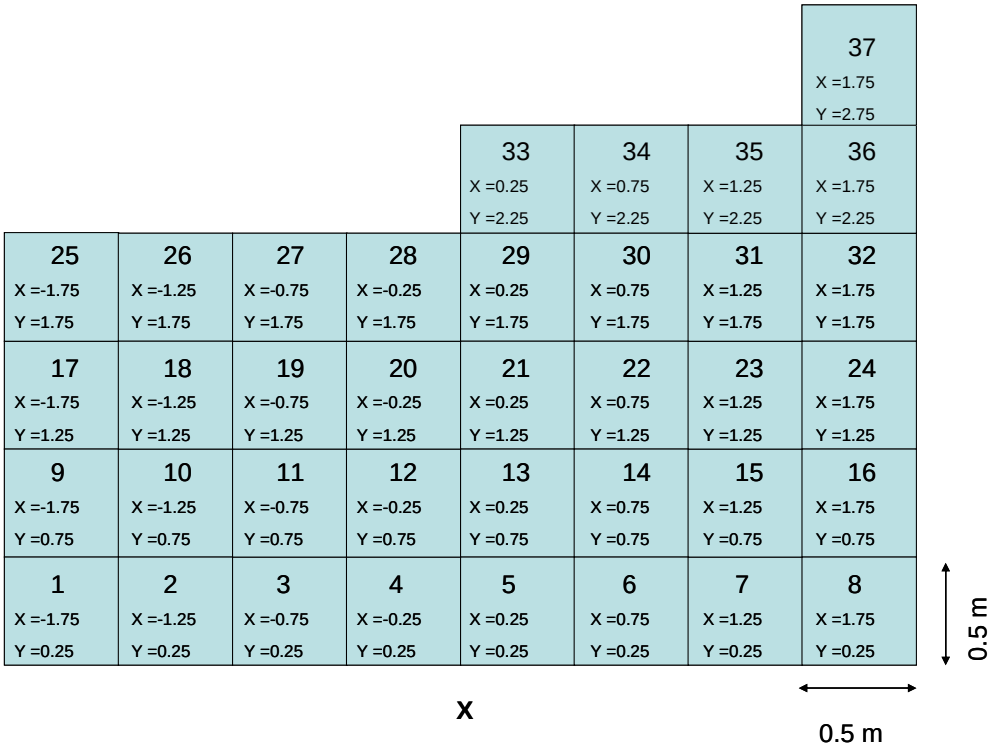

Figure G 34 Plan view of the grid layout across Impala P3 for Boussinesq evaluation. The origin is the centre of the bottom (down-dip) edge. The bold "X" position represents the approximate position of the first stress measurement

G5 Union Spud-shaft

G5.1 Stress change measurements (section and plan view)

Measurements were conducted over an isolated pillar, specially cut for instrumentation purposes. The site offered a unique opportunity of measuring pillar stress without the interference of adjacent pillars or the unknown effects of gullies on pillar behaviour. Closure and stress change instrumentation were installed over the abutment at the edge of the ledged centre gully at the proposed

position of the pillar (Figure G 35). Shallow dipping boreholes were drilled in the positions shown by P1a and P1b in the figure and 2D stress cells were installed at 3.4 m and 5.4 m above the pillar respectively. The boreholes and cell locations are shown in section in Figure G 36. P1a was installed 0.5 m away from the pillar edge (over the ledge) and P1b was 0.9 m in from the edge (over the pillar) in plan.

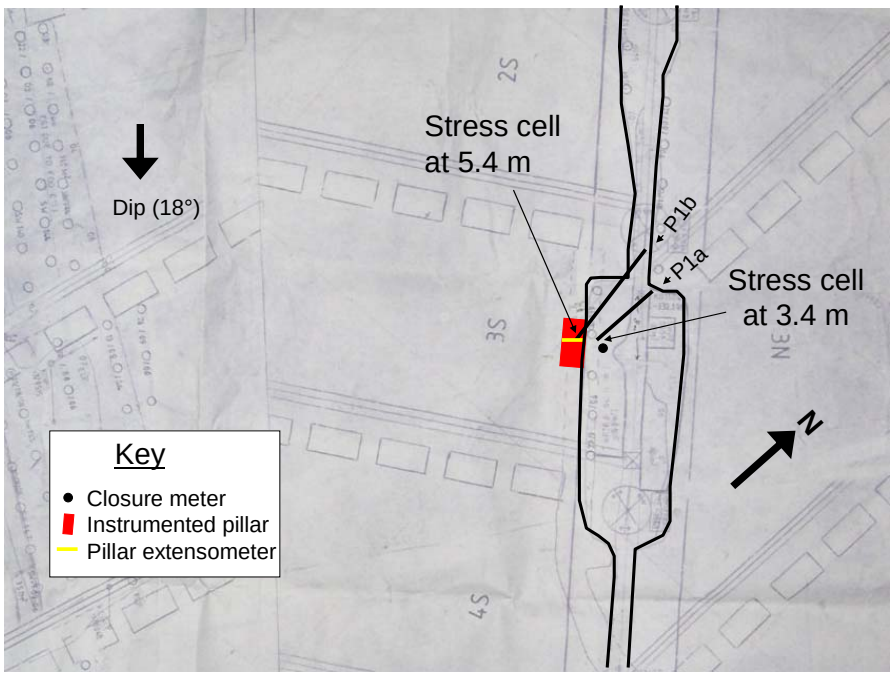

Figure G 35 Stope sheet showing the ledged centre-raise and proposed position of Union P1

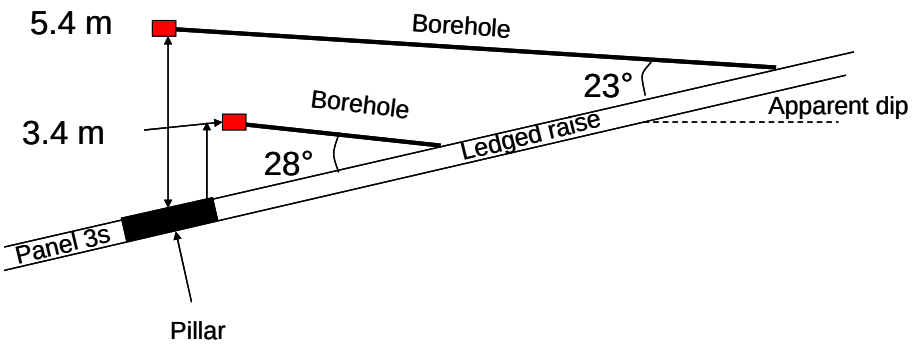

Figure G 36 Section showing the stress cell locations (P1a and P1b) relative to the pillar (not drawn to scale)

As the pillar was additional to the normal pillar configuration, it was cut to smaller than standard dimensions to determine the feasibility of using such dimensions in the future. The important issues were the peak strength as the current pillars often damage the hangingwall in poor rock mass conditions, and the residual strength during the working life of the stope as the pillars must prevent parting on the Bastard Reef some 20 m to 25 m above. Unfortunately the stoping width on the south side of the pillar (Figure G 35) was not consistent along the length of the pillar, which may have had a slight effect on strength. The final pillar dimensions were about 2.8 m x 5.8 m and an average height of about 1.5 m, i.e. w/h of 1.9. The pillar was oriented with its long axis on dip as shown in Figure G 35. The pillar failed when the mining reached the configuration shown by the pink in Figure G 37, before being properly formed. A 2 m wide end was advanced up the back of the pillar after failure to hole into the up-dip “half-panel”, as shown by the orange rectangle. Subsequently, mining was advanced in a breast configuration to the final face position, where mining was terminated due to poor ground conditions. In Figure G 37, monthly face advances are represented by an array of colours and the pillars and unmined areas are shown as grey. Boreholes were drilled after mining was complete in the panel to monitor the residual stress change (P1c) and the residual stress profile (P1d). The locations of these boreholes are also plotted in Figure G 37. Sections showing the orientations of Boreholes P1c and P1d relative to the pillar are provided in Figure G 38 and Figure G 39 respectively.

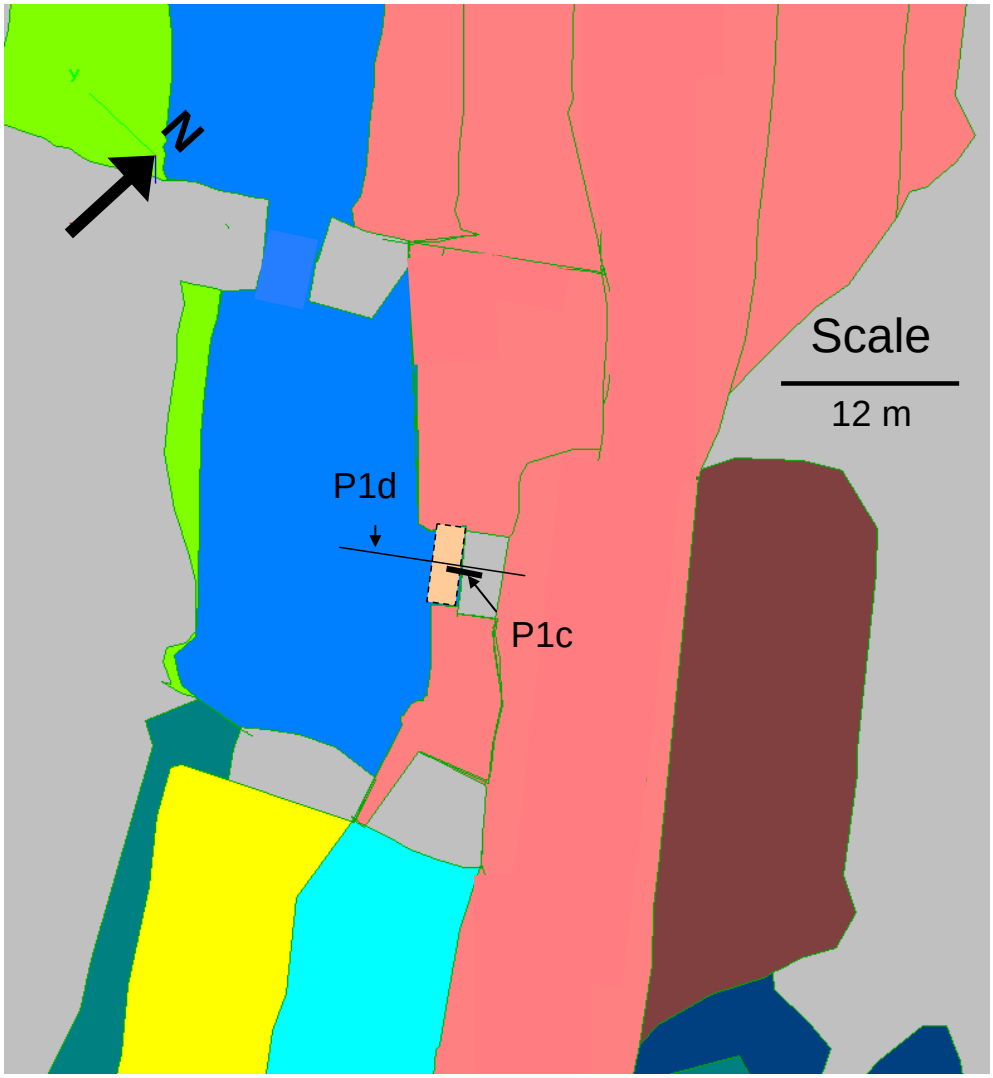

Figure G 37 Stope sheet showing the monthly face advances, approximate positions of the stress change (P1c) and profile (P1d) boreholes over the instrumented pillar

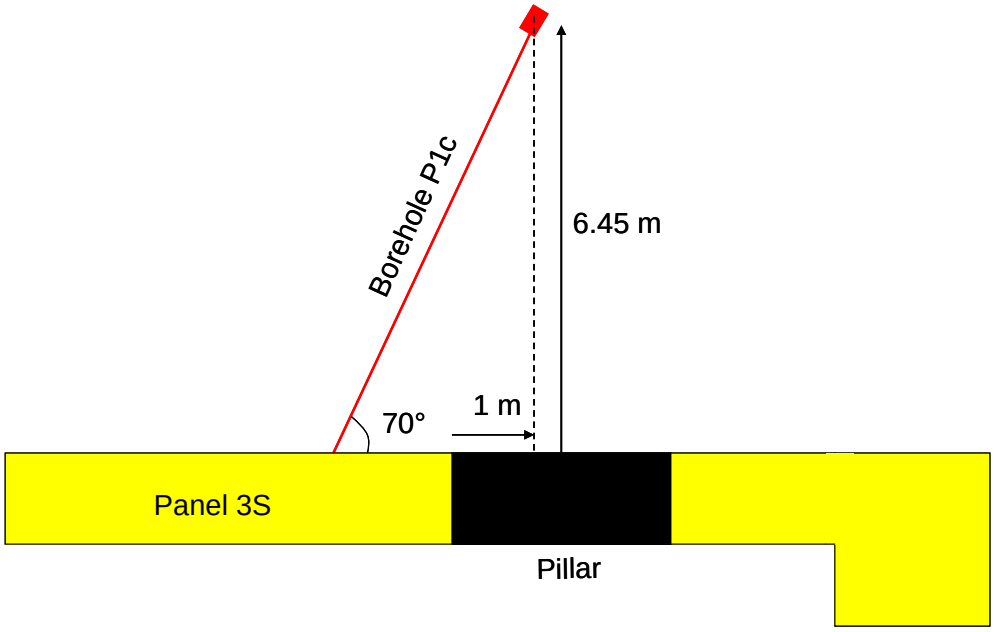

Figure G 38 Section showing Borehole P1c over Union P1 (not drawn to scale)

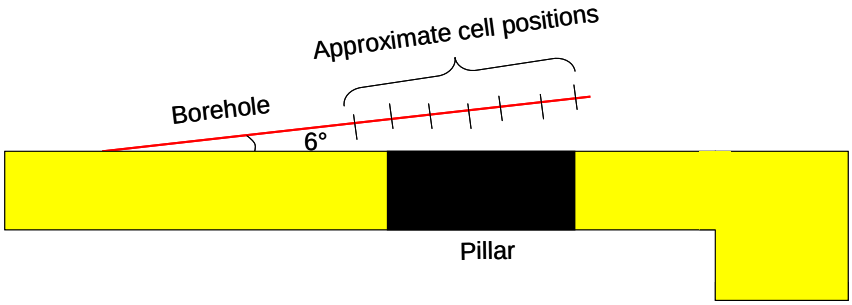

Figure G 39 Section showing the borehole used to conduct the stress profile measurements (P1d) over Union P1 (not drawn to scale)

The stress measurements in P1d ranged in height from 1.4 m to 1.9 m above the pillar. The intention was to measure vertical stress with a set of closely spaced cells. However, an obliquely oriented, vertical discontinuity at about 8.7 m prevented some measurements from being done. A series of seven 2D measurements were conducted over the pillar and stope on either side of the pillar. In addition, 3D measurements were conducted at much greater heights

(4.66 m and 5.38 m) in Borehole P1c. These measurements allowed a much broader overview of the stress condition of the whole pillar, by virtue of their height above the pillar. The stresses measured in the boreholes represented a fraction of the stress on the plane of the top contact of the pillar. Thus the stress distribution across the pillar itself was calculated using an inverse matrix of Boussinesq equations (Poulos and Davis, 1974), based on the measurements in the boreholes. A plan view of the Boussinesq co-ordinate system used across the top boundary of the pillar is shown in Figure G 40. The pillar was divided into 0.56 m x 1.16 m blocks as shown in the figure.

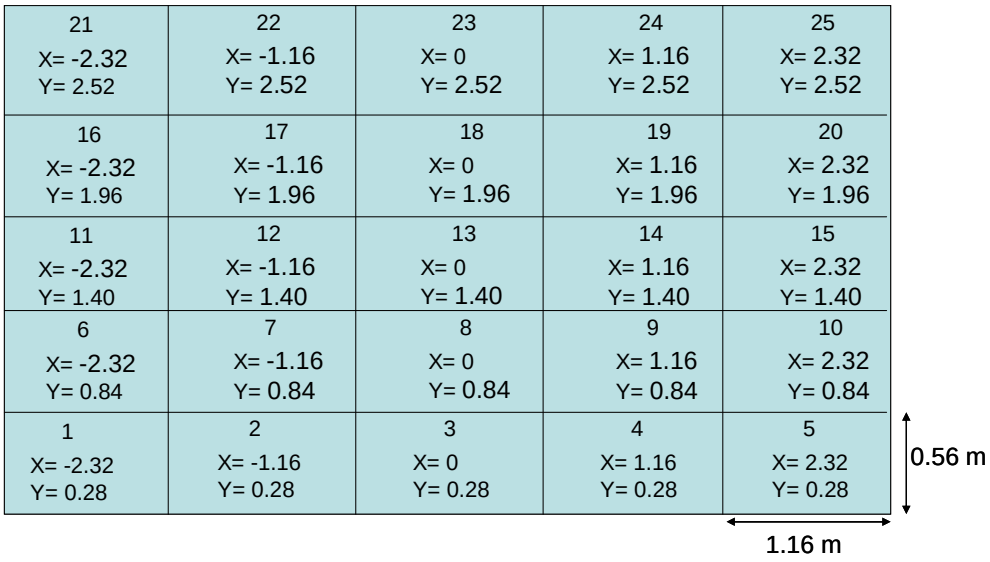

Figure G 40 Plan view of the grid layout across Union P1 for Boussinesq evaluation. The origin is the centre of the bottom (down-dip) edge

The borehole breakout shown in Figure G 41 was observed in the inspection hole prior to any mining in the stope (Figure G 35). The high angle of 42° suggests an unexpected orientation of the major principal stress in the plane normal to the borehole axis. The orientation of the breakout in the extensometer borehole, located 0.42 m down-dip of the inspection hole, was oriented at 26° in the opposite direction, i.e. 68° to each other. The borehole breakout in the extensometer borehole suggested that the major stress was almost normal to the reef at this position. The abrupt change in orientation of the major stress

highlights the difficulties of determining the pillar stress from stress measurements at the Union site.

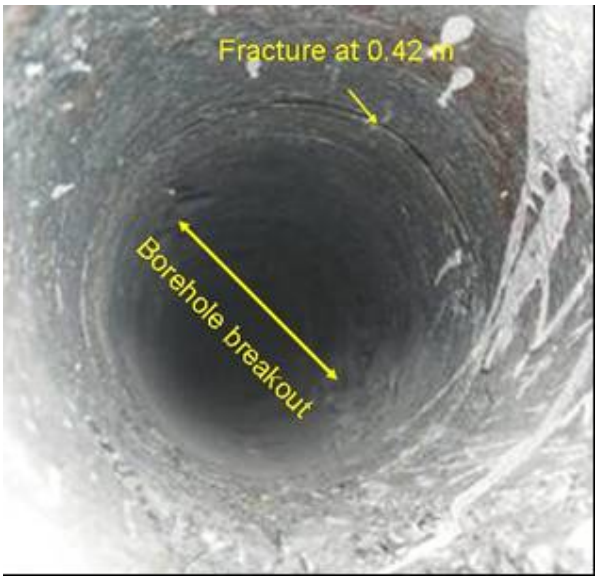

Figure G 41 Fracturing and slight borehole breakout observed in the Union P1 sidewall inspection borehole, drilled adjacent to the extensometer

G6 References

COMRO. (1981). MINSIM-D User's Manual, Chamber of Mines of South Africa, Johannesburg, RSA.

Poulos, H.G. and Davis, E.H. (1974). Elastic solutions for Soil and Rock Mechanics, New York: J Wiley and Sons, pp. 424.

Roberts, D.P., Canbulat, I. and Ryder, J.A. (2002). Design parameters for mine pillars: strength of pillars adjacent to gullies; design of stable pillars with w/h ratio greater than 6; optimum depth for crush pillars, *SIMRAC GAP617 Final Report,* The Safety in Mines Research Advisory Committee (SIMRAC), Braamfontein, RSA.